NON-STATIONARY IMPEDANCE ANALYSIS OF LEAD/ACID BATTERIES

Z. STOYNOV*, B. SAVOVA-STOYNOV and T. KOSSEV

Central Laboratory of Electrochemical Power Sources, Bulgarian Academy of Sciences, Sofia 1040 (Bulgaria)

Introduction

In recent years, a series of papers has been devoted to the impedance study of lead/acid batteries. Following the first successful measurements on commercial batteries [1], a number of papers have been concerned with the analysis of large-size batteries or their separate electrodes [2 - 4], as well as with the modelling of systems imitating different properties of real batteries [5, 6].

Impedance studies have several objectives including: determination of electrochemical mechanisms and their adequate impedance models; estimation of the external electrical parameters of the battery as a power source; technological control of product quality.

The impedance study of lead/acid batteries is beset by difficulties that are caused by the complex nature of the processes involved. From the system point of view, the batteries are non-linear, multi-parameter, quasi-irreversible, large statistical systems with distributed parameters on both the macro- and the micro-scale. Processes of energy and mass transport take place in the batteries that cause significant changes in the internal microstructure and operational behaviour.

Many simplifications are necessary in order to achieve a successful impedance study of a lead/acid battery. The first problem is the linearization of the system parameters. The choice of the a.c. value of the current/voltage should be a compromise between the general requirement for small signal deviation (SSD) and data quality that is directly related to the amplitude of the a.c. signal. On the other hand, a large a.c. signal decreases the non-stationary errors. In this context, it is instructive to mention the experimentally established fact that lead/acid batteries behave as quasi-linear systems over a very wide range of perturbation deviations [7].

The study of the battery as a system has practical importance, but cannot be used for discovering the mechanisms of the reactions taking place within the battery. In previous experimental work [1], it was shown that the

*Author to whom correspondence should be addressed.

0378-7753/90/$3.50

different electrodes of the lead/acid battery have significantly different impedances, whereby summation of the impedance diagrams is impossible.

The non-stationary state of the battery causes more serious difficulties. Attempts to measure the impedance of the separate electrodes in a steady state, *i.e.*, after switching off the current and after a certain relaxation time, have proved unsuccessful because the processes occurring during this period are quite different from those taking place during the normal electrode operation. This is the main reason why the results obtained usually do not give any useful information about the basic processes occurring during the charge or discharge. Therefore, it has been suggested [2, 8] that impedance measurements should be carried out *in situ*, *i.e.*, under passage of current during the course of battery charge/discharge. This approach has now been accepted and at present is considered to be the standard procedure.

Using the *in situ* method, the problem of errors caused by the non-stationary behaviour of the battery is intensified. The first and simplest solution to this problem is the quasi-stationary approach. This assumes that the errors caused by the non-stationary conditions are negligible and that the system can be considered to be stationary during the measurement period [1]. All present studies of the impedance of lead/acid batteries follow this philosophy.

To apply the quasi-steady-state (QSS) approach, it is necessary to develop a method for estimating the non-stationary errors. It has been shown [7] that these errors depend on both the system variability (*i.e.*, on the deviations of the impedance and the potential of the system) and the amplitude of the measuring signal. Since the errors increase sharply with decrease in frequency, they greatly limit the applicability of low frequencies at which, unfortunately, many interesting phenomena occur [2].

Another important and dominant error arises from the 'frequency by frequency' mode of the impedance measurement method itself, where the system changes greatly within one frequency sweep, and its final state differs significantly from the state at which the measurement was commenced. The resulting impedance diagram is a sum of different states, and therefore cannot be interpreted as an impedance in the classical sense. It has been shown [10] that this error can be estimated and corrected.

Four-dimensional method for non-stationary impedance analysis

The method of four-dimensional (4D) non-stationary impedance analysis is based on a consecutive measurement of a series of impedance diagrams in a given frequency range.

From the experimental data, a 4D array can be formed:

$$D(Re_{ij}, Im_{ij}, t_{ij}, w_i) \quad (1)$$

where: w_i are the measurement frequencies; Re_{ij} and Im_{ij} are the impedance components corresponding to w_i for the ith measurement; t_{ij} is the time for

each measurement. These data contain information on the frequency behaviour of the system as a whole in the course of its evolution.

The correction of the errors caused by the system evolution is based on the hypothesis that the state and parameter spaces of the system are in a continuum. With this assumption, each projection of these spaces can be described by a given formal mathematical model that satisfies the requirements for the continuum. By means of this approximation model, an interpolation can be performed for the given time, t_j, and frequencies, w_i, and the estimates of the real and imaginary parts of the impedance diagrams can be obtained, *i.e.*,

$$\hat{\mathrm{Re}}_{ij}^{*} = \mathrm{Spl}^{-1}\{S_{i,\,\mathrm{Re}}/t_j\} \tag{2}$$

$$\hat{\mathrm{Im}}_{ij}^{*} = \mathrm{Spl}^{-1}\{S_{i,\,\mathrm{Im}}/t_j\} \tag{3}$$

where Spl is the approximating cubic spline.

Using the above spline approximation, the real and imaginary parts can be estimated and a set of corrected impedance diagrams generated:

$$\hat{Z}_j(w_i, \hat{\mathrm{Re}}_i^{*}, \hat{\mathrm{Im}}_i^{*}) \tag{4}$$

The diagrams can be interpreted as instantaneous impedance diagrams, *i.e.*, instantaneous projections of the non-stationary transfer function of the system, or as 'frozen' stationary states of the system. This method is described in detail in ref. 10.

Experimental

Test equipment

Measurements of the impedance of real lead/acid batteries in accordance with the 4D approach require power galvanostats and software for control of the experiment; these are not commercially available. For this purpose, the battery impedance facility [11] has been renewed and remodeled around the Frequency Response Analyzer Solartron 1174, and a front-end computer (Tektronix 4051) connected via a standard interface (RS232) to a central computer (IBM/AT). The front-end computer executes the full control of the impedance measurements, monitors and stores, temporarily, the results, and transfers them to the central computer. The measurement part of the facility is coupled with a home-made power galvanostat (30 A, 20 V) with a phase shift error of the control transfer function (from the input sinusoidal signal to the current) of 3° at 10 kHz.

The second part of the instrumentation is a precise measurement, double-differential amplifier–signal conditioner that has been calibrated carefully to minimize the cross-channel errors, and stabilized to values less than 0.1° at 10 kHz. This accuracy is equal to that of the Solartron analyzer. An additional device has been interfaced via IEEE488 to the front-end computer

and provides precise measurement of the d.c. potential and external d.c. bias correction, as well as the exact time of every frequency point.

A second computerized system operates the cells under investigation during the plate formation process and the cycling tests. This system includes power-testing equipment 'Betatest' 140 M (*i.e.*, galvanostat 100 A, double potentiostat for battery protection, thermoregulator of the bath and cell thermometers), fully controlled by an 8-bit Apple-2 system. The computer control of the process of plate formation and cycling has the advantage of precise and reproducible preconditioning of the cell. This is essential for comparative impedance studies because the 'memory' effect of lead/acid batteries demands well-defined and long-term reproducible preconditioning procedures.

The battery studied was a standard 140 A h, 12 V traction pasted-plate type. Container formation of the 6 cells was carried out for 40 h in accordance with the manufacturer's specifications. After formation, the electrolyte was changed for one of the nominal density and the cells were discharged galvanostatically at 28 A down to 1.7 V/cell. From the records of the individual voltage/time dependencies and the cell capacities, one cell (A01) with nominal characteristics was selected for the impedance measurements. All measurements were performed on the negative electrode by means of a standard mercury/mercurous sulphate reference electrode. All potentials are reported with regard to this electrode.

Impedance measurements

Impedance measurements of the negative electrode of the A01 cell were carried out during the first charge immediately following the first discharge. The other 5 cells were charged at the same current (10 A) in order to monitor the reproducibility. The amplitude of the a.c. galvanostatic current was kept at 2 A_{eff}, giving voltage deviations in the range 5 - 25 mV.

Five minutes after the beginning of charge, the first impedance diagram was measured from 1 kHz down to 3.97 mHz (5 points per decade) with automatic recording of the electrode potential and time of commencement of the impedance measurement, as well as the time at completion of the measurement. Every 30 or 60 min, a new diagram was measured in the same manner and at the same frequencies. During the charge, 17 diagrams were obtained in total.

Data processing

All the data were pre-processed in the following way:

(i) Control of data quality

This control was carried out over each registered impedance diagram in accordance with the method described in ref. 12. Only the points at 100 Hz from each diagram were qualified as 'low quality', but in order to maintain the completeness of the sweep, these points were neither rejected nor corrected.

(ii) Correction of the shunt and cell self-inductances

Before the experiment, the shunt self-inductance was evaluated as an additive lumped parameter of 13 nH by measurement with an external resistor (second shunt) of known real resistance [13]. The data were corrected for this value; this correction was significant only for frequencies above 100 Hz. By independent measurement of the cell impedance up to 10 kHz, the cell self-inductance was evaluated as 25 nH. All the impedance diagrams were corrected for the presence of this parameter.

The final data processing was performed according to the 4D method described above. As expected, significant corrections were observed in the diagrams that corresponded to the most rapid changes in the potential. The importance of this 4D correction can be seen in Fig. 6(a) and (b) (see below), where a significant improvement in the impedance diagrams is observed. After the correction, the depression of the semi-circles decreases: the transition region between the two last semi-circles becomes sharp and clear and the unreasonable point at the lowest frequency disappears in the corrected diagram.

Results

Figure 1 gives a representative set of corrected impedance diagrams, together with the potential development, in a 3-dimensional space, as a function of the time of charge. The results show that the total electrode impedance changes significantly: it increases from a value of ~ 2 to ~ 12 mΩ and then decreases to 7 - 8 mΩ. This behaviour corresponds roughly to the derivative of the potential–time dependence. Fine details that could not be detected from the potential measurement are present in the individual impedance diagrams. All these diagrams can be grouped into three regions corresponding to the state-of-charge, namely:

(i) a region at the beginning of charge where the state-of-charge is $\leqslant 30\%$; the impedance is low and develops slowly;

(ii) a transition region where the fastest changes in potential occur and where $s = 30 - 75\%$; the impedance increases and alters significantly in behaviour;

(iii) a region where the potential becomes stabilized ($s > 75\%$) and where intensive gassing of the cell can be observed; the impedance decreases and also tends to stabilize.

It is difficult to construct a quantitative model that is capable of fitting all the above data numerically. Valuable qualitative conclusions can be made, however, by examining the individual impedance diagrams.

The first diagram, measured 35 min after the beginning of charge, is shown in Fig. 2. The impedance consists of two well-pronounced loops — a 'positive' one and a 'negative' (pseudo-inductive) second loop. This general shape is maintained in a series of consecutive diagrams following the first one. As a matter of fact, the pseudo-inductive loop is composed of a negative

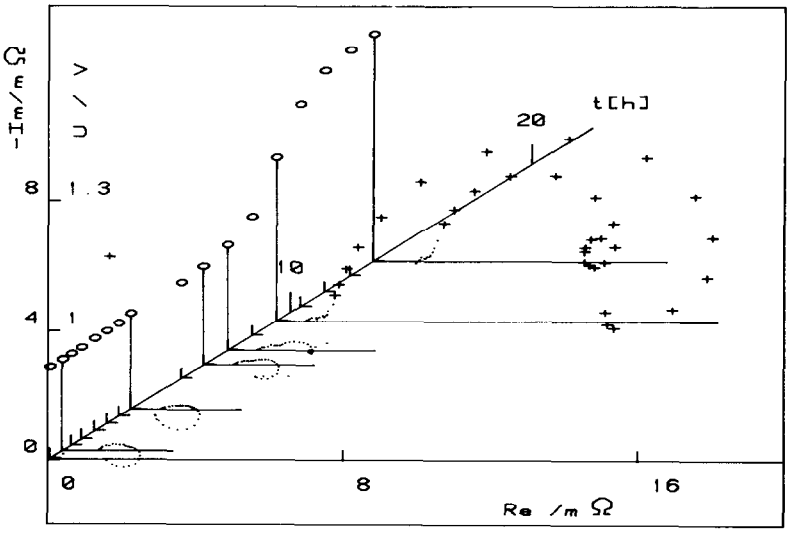

Fig. 1. Three-dimensional plot of (+) impedance and (○) potential development of negative electrode during charge (140 A h traction battery of pasted-plate type) at 10 A.

resistance and a negative capacitance [13]. Thus, the shape can be attributed to consecutive endothermic and exothermic processes. Taking into account this structure, and also knowledge of the processes during charging of the negative plate, it can be concluded that the impedance diagram represents the processes of crystallization of the negative paste. The positive loop is associated with the process of nucleation and the exothermic loop with the process of propagation.

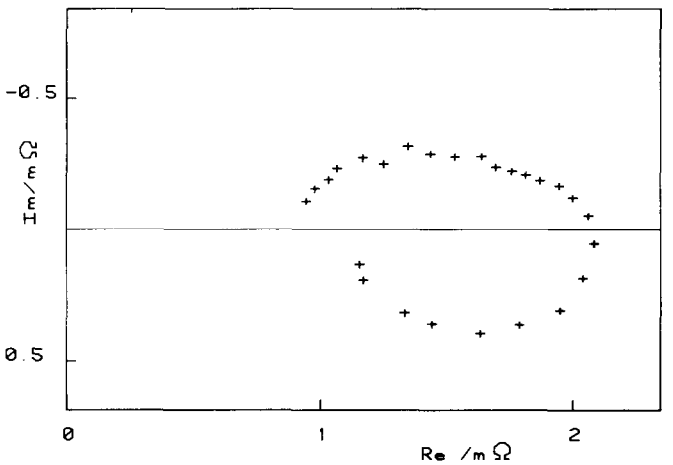

Fig. 2. Impedance diagram of negative electrode 35 min after beginning of charge: $f_{max} = 1$ kHz, $f_{min} = 3.97$ mHz, 5 p/dec.

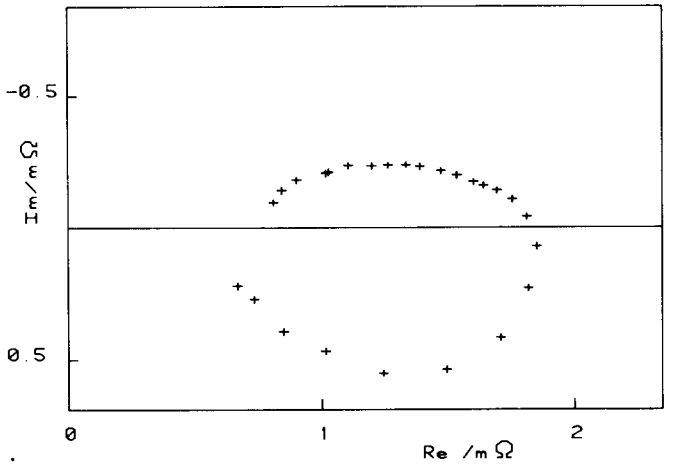

Fig. 3. Impedance diagram 205 min after beginning of charge at same frequencies as in Fig. 2.

Qualitative analysis of the diagrams given in Figs. 3 and 4 reveals that the positive loop is, in fact, a doublet, *i.e.*, another reaction precedes the process of nucleation. During charging, this prior reaction becomes more and more pronounced; the barrier for nucleation decreases slightly, while the resistance corresponding to the exothermic loop increases at first (Fig. 3) and then decreases to very small values (Fig. 5). This loop shows some unusual behaviour at the lowest frequency (Figs. 2 - 4). By studying the evolution, however, it can be concluded that this behaviour is due to the presence of another loop which is, at first, difficult to observe but becomes more pronounced (Fig. 5) and then starts to dominate after a few hours (Fig. 6). This

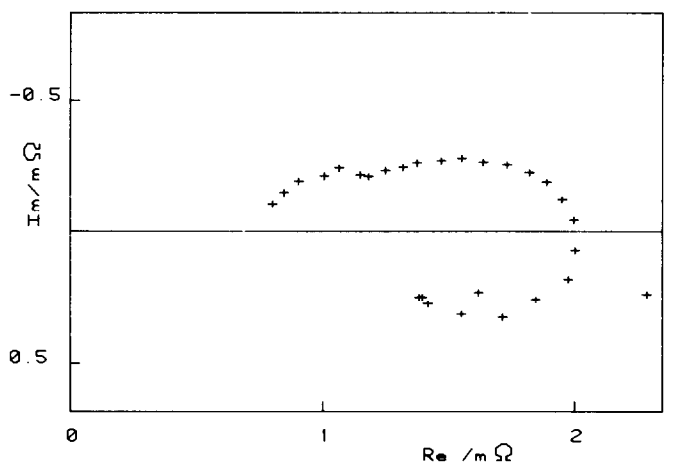

Fig. 4. Impedance diagram 385 min after beginning of charge at same frequencies as in Fig. 2.

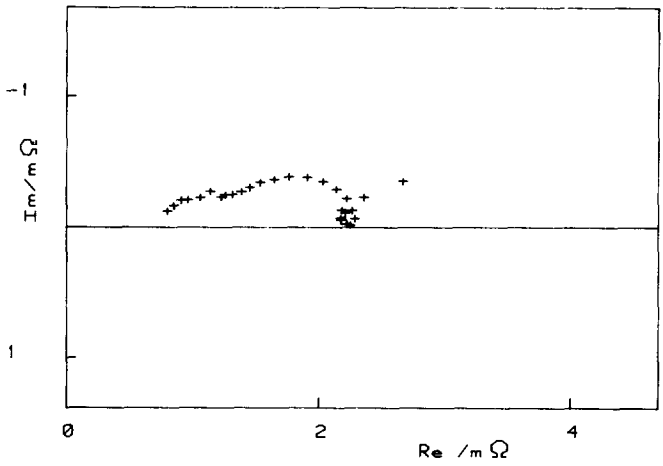

Fig. 5. Impedance diagram 445 min after beginning of charge at same frequencies as in Fig. 2.

last phenomenon could possibly be due to the further growth of the already-formed crystallites.

With continued charging, the impedance increases as a whole effective resistance and, under the galvanostatic current, the potential of the electrode increases. The potential eventually reaches the stage of hydrogen-gassing activation. At this point, the impedance reaches a maximum value, but totally changes its shape (Fig. 7). This behaviour is due to the parallel connection of two parts representing a double-current pathway, namely, an increasing impedance corresponding to the crystallization process and a decreasing impedance corresponding to hydrogen evolution.

It should be noted that one part of the new composite shape maintains the form of a semi-circle: obviously the process of hydrogen evolution is very active and takes place on the surface of the electrode without going deep into the pores. By contrast, very low frequencies that can penetrate to the bottom of the pores, emphasize the continuous process of the new phase formation. Even after reaching the potential plateau where the component of the impedance corresponding to hydrogen evolution decreases (Fig. 8), the competing charging process is still in progress. It is clear that the hydrogen evolution activity depresses the charging process; this is to be expected. A more important result is the fact that attainment of the potential plateau does not signify the end of the charging process.

Discussion

The above studies show that 4D analysis is a powerful technique for understanding impedance data gathered on real lead/acid batteries. Careful

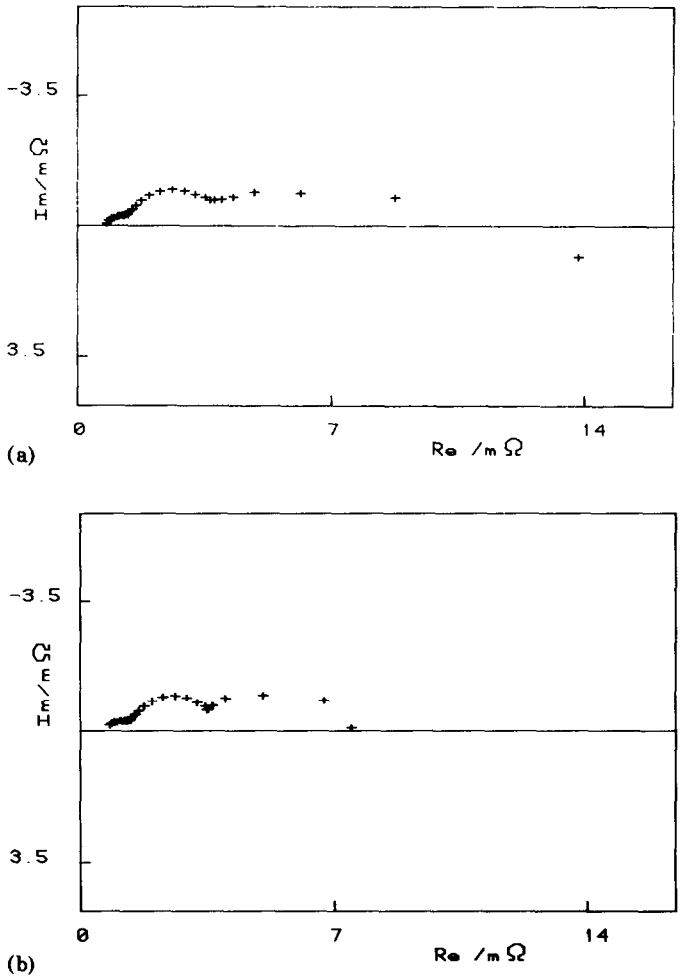

Fig. 6. Impedance diagram 505 min after beginning of charge at same frequencies as in Fig. 2. (a) uncorrected raw data; (b) 4D and L corrected diagram.

design of experiments, precision in measurement, and data pre-processing are essential criteria for achieving successful results.

Some general conclusions can be drawn from the experimental results to date. The first concerns the porosity of the negative paste. Clearly, for the battery examined, the porosity of the negative paste was high, the pores were large and short and the accessible frequencies of a few millicycles were sufficient to reach the bottom of the pores and to sense the processes taking place there. The nature of these processes leads to the second important conclusion. The recorded impedance shapes corresponding to the first stage of plate charging can be related to crystallization processes. It should be remembered that the analysed cycle is for the initial charge and it is possible

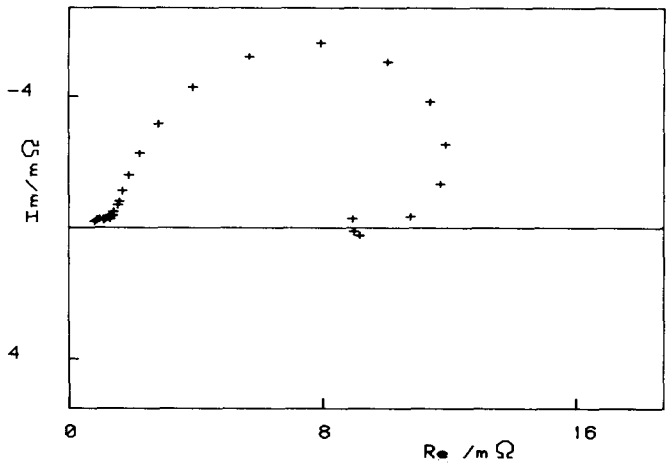

Fig. 7. Impedance diagram 565 min after beginning of charge at same frequencies as in Fig. 2.

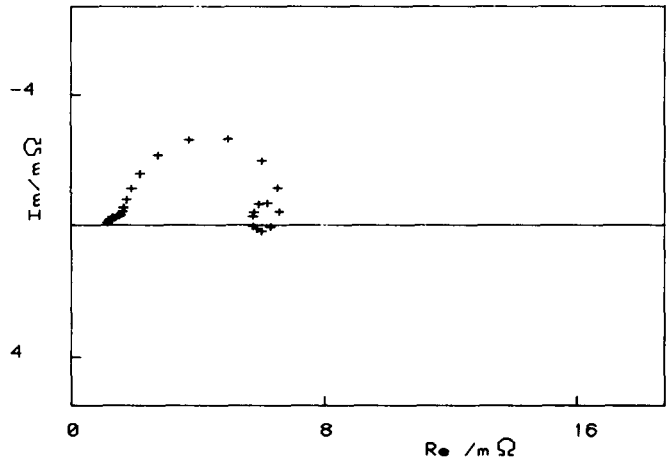

Fig. 8. Impedance diagram 806 min after beginning of charge at same frequencies as in Fig. 2.

that the process of plate formation is not finished and is still taking place during this process. In this connection, it will be very interesting to follow the impedance evolution during the next cycles. This task is, however, beyond the scope of this work and will be considered separately.

The evolution of the impedance observed during charging shows an interesting development in the phenomena that could not be detected by simple d.c. measurements. It appears that the study of the impedance cycling evolution of the negative, and also of the positive electrodes, could supply valuable information for elucidating the dynamics of the processes taking place in lead/acid batteries.

References

1 M. Keddam, Z. Stoynov and H. Takenouti, *J. Appl. Electrochem.*, *7* (1977) 539.
2 Z. Stoynov, *Ext. Abstr., 28th ISE Meeting, Varna, 1977*, p. 148.
3 N. A. Hampson, S. A. G. R. Karunathilaka and R. Leek, *J. Appl. Electrochem.*, *10* (1980) 3.
4 S. Sathyanarayana, S. Venugapalan and M. L. Gopikanth, *J. Appl. Electrochem.*, *9* (1979) 125.
5 C. Rakotomavo, *Dissertation thesis*, Paris, 1983.
6 Л. А. Бекетаева and Рыбалка К. В., Имледанс активой массы отриатель-ных электродов свинцового аккумулятора, Электрохимия, т. XXII, вып. 3, 1986.
7 O. Nakamura, S. Higuchi, S. Okazaki and S. Takahashi, *J. Power Sources*, *17* (1986) 295.
8 Z. Stoynov, *Ext. Abstr. II, 29th ISE Meeting, Budapest, 1978*, p. 833.
9 Z. Stoynov and B. Savova, *J. Electroanal. Chem.*, *112* (1980) 157.
10 Z. Stoynov and B. Savova, *J. Electroanal. Chem.*, *183* (1985) 133.
11 Z. Stoynov and B. Savova, *Ext. Abstr., 32nd ISE Meeting, Dubrovnik, 1981*, p. 650.
12 Z. Stoynov and B. Savova, *Ext. Abstr., 166th AES Meeting, New Orleans, 1984*, p. 159.
13 Z. Stoynov and B. Savova, *J. Electroanal. Chem.*, *170* (1984) 63.